The International Journal of Advanced Manufacturing Technology (2019) 100:2387–2399
https://doi.org/10.1007/s00170-018-2838-4

ORIGINAL ARTICLE

Analysis of flatness control capability based on the effect function and roll contour optimization for 6-h CVC cold rolling mill

Hongbo Li[1] · Zhenwei Zhao[1] · Jie Zhang[1] · Ning Kong[1] · Renren Bao[1] · Shenghui Jia[2] · Fei He[3]

Received: 9 May 2018 / Accepted: 3 October 2018 / Published online: 16 October 2018

Abstract

The 6-high continuously variable crown (6-h CVC) cold rolling mill shows limited capability to control coupled edge and center waves for both narrow strip and ultra-wide strip production. In order to solve this problem, an integrated three-dimensional (3D) elastic-plastic finite element model (FEM) of rolls and strip is built to calculate the effect functions in consideration of work roll bending (WRB), intermediate roll bending (IMRB), and CVC intermediate roll shifting (IMRS) with different strip widths. A set of orthogonal vectors which is defined as eigenvectors is proposed to analyze the similarities and the complementarities of the effect functions. It is applied to study the flatness control characteristics of the cold rolling mill. Based on the analysis of flatness stress characteristics of different strip widths in the production, it is found that the similarities between the flatness stress and the eigenvectors of different strip widths are relative low. The flatness defects are difficult to be eliminated. From the relationship between IMRS and strip widths, a segmented CVC intermediate roll contour is then proposed and experimented in an industrial production. The proportion of coupled edge and center waves is decreased by 15.2%, and the overall flatness is reduced by 0.7 IU.

Keywords 6-h CVC cold rolling mill · Effect function · 3D FEM · Flatness control · Roll contour

1 Introduction

Continuously variable crown (CVC) mill has been extensively employed to more than 150 production lines around the world since it was developed in 1982. It is one of the most important mill type for the tandem cold mills [1]. 6-high continuously variable crown (6-h CVC) cold rolling mill was developed and successfully applied in practice production by Schloemann-Siemag (SMS), Germany [2]. As a new generation cold rolling mill, it is installed with many flatness control methods, such as work roll bending (WRB), intermediate roll bending (IMRB), CVC intermediate roll shifting (IMRS), roll tilt (RT), and roll sectional cooling (RSC) [3, 4]. It provides strong flatness control capability, which is suitable for cold rolling production of the ultra-wide strip [5, 6].

Two thousand one hundred eighty millimeters of 6-h CVC cold rolling mill production line which is consist of five stands is mainly applied to the production of car body plates and other high-grade appliances strips. It possesses the longest roll body and produces the maximum width rolled strip, which covers the largest range of strip widths and the largest width to thickness ratio for a cold rolling mill. Besides, the cold rolling mill is equipped with advanced flatness detection equipment, abundant flatness control methods, and advanced flatness control model [7, 8]. However, in practice production, such advanced cold rolling mill is still difficult to eliminate the coupled edge and center waves for both narrow strip (strip width B is about 1000~1300 mm), as shown in Fig. 1a, and ultra-wide strip (strip width B is about 1600~2000 mm), as shown in Fig. 1b. It affects the quality of follow-up products during cold rolling and the stability of production process. By collecting and analyzing the process parameters of practice production, such as WRB, IMRB, IMRS, RT, and RSC et al., it is found that the cold rolling mill does present some limitations for controlling the typical flatness defects in

✉ Hongbo Li
lihongbo@ustb.edu.cn

[1] School of Mechanical Engineering, University of Science and Technology Beijing, Beijing 100083, People's Republic of China

[2] Wuhan Iron and Steel(Group) Corp, Wuhan 430083, People's Republic of China

[3] Collaborative Innovation Center of Steel Technology, University of Science and Technology Beijing, Beijing 100083, People's Republic of China

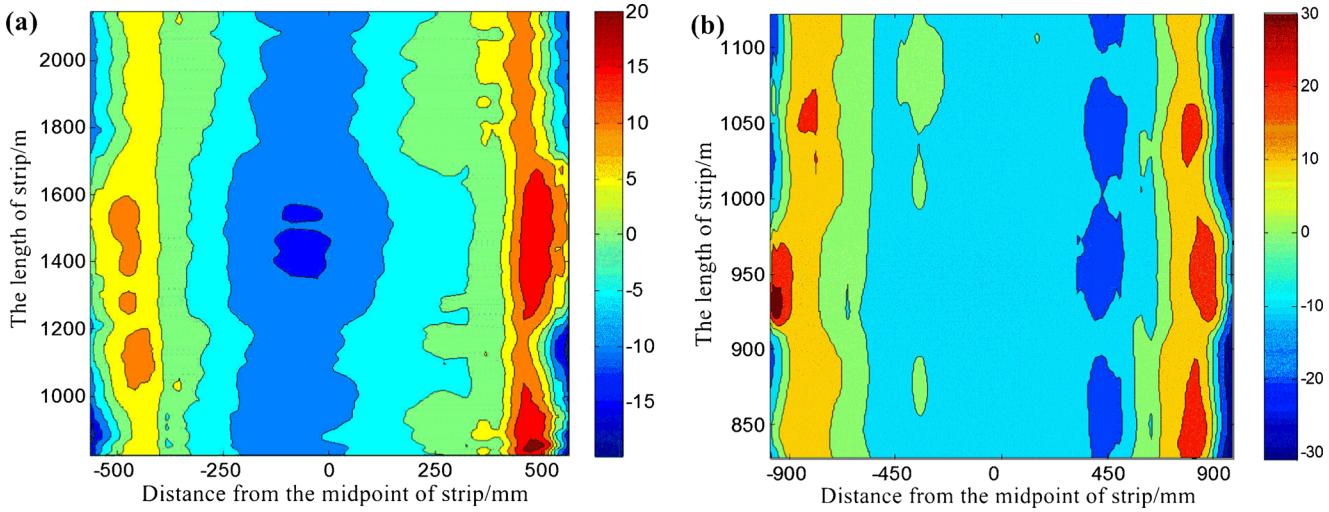

Fig. 1 The internal stress nephogram of different strip widths: **a** The strip width is 1050 mm and **b** the strip width is 1990 mm

narrow strip and ultra-wide strip production. Yang et al. [8] built a three-dimensional (3D) finite element model (FEM) to analyze the effect of different stands on flatness control for a 6-h CVC cold rolling mill. The results showed that the control capability was not sufficient to eliminate the coupled edge and center waves. Bao et al. [9] analyzed the influence of asymmetric flatness of different strip widths in the rolling process and pointed out that edge waves were more likely to be caused when the strip was running in the annealing furnace. So, it is indispensable to analyze the control capability and address the problem of typical flatness defects with different strip widths in a 6-h CVC cold rolling mill.

The flatness control performance of the cold rolling mill is analyzed in order to analyze the feasibility and effectiveness of the cold rolling mill on the control of typical flatness defects. Generally, the analysis of flatness control capability is based on the roll gap crown method [10–12]. It can be used to calculate the range of secondary crown and quartic crown of WRB, IMRB, and IMRS in different strip widths in order to evaluate its flatness control capability. Rosenthal and Bald et al. [13, 14] used this method to analyze the control capability of a 6-h CVC cold rolling mill. However, on the one hand, simply increasing the CVC roll gap crown range to expand the mill roll gap crown has failed to adequately address flatness problem in the production. On the other hand, adopting crown to characterize strip profile cannot accurately describe the adjustment characteristics of a control method along the strip width. The similarity and complementarity between different control methods cannot be analyzed and compared as well. Another method is based on the effect function [15, 16]. Liu et al. [17] applied this method to a 900-mm HC 6-high mill for cold rolling strip and provided a theoretical framework for flatness control. Song et al. [18] used this method and high-order Legendre polynomial function to establish the dimensionality reduction efficiency inherited regulation method and the two-loop comprehensive regulation control model. Yan et al. [19] used this method to analyze the control capability of 1200 mm narrow strip for a 2180-mm tandem cold rolling mill, and the work roll contour optimization was proposed to solve the control problem for narrow strip flatness. However, the roll contour was only suitable for a certain strip width and cannot simultaneously address the problem of strip flatness for both narrow strip and ultra-wide strip.

Many efforts have been made to further grasp the flatness control capability of the cold rolling mill during rolling process [20, 21]. Lu et al. [22] proposed a design method of a third-order CVC roll profile. Li et al. [23] designed the new asymmetry self-compensating work roll contour and the flatness control

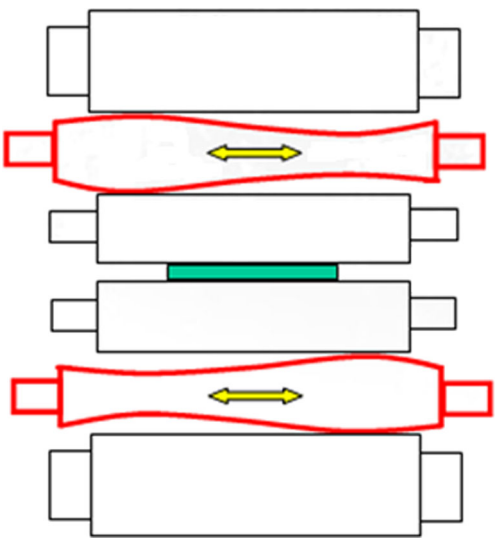

Fig. 2 6-h CVC cold rolling mill

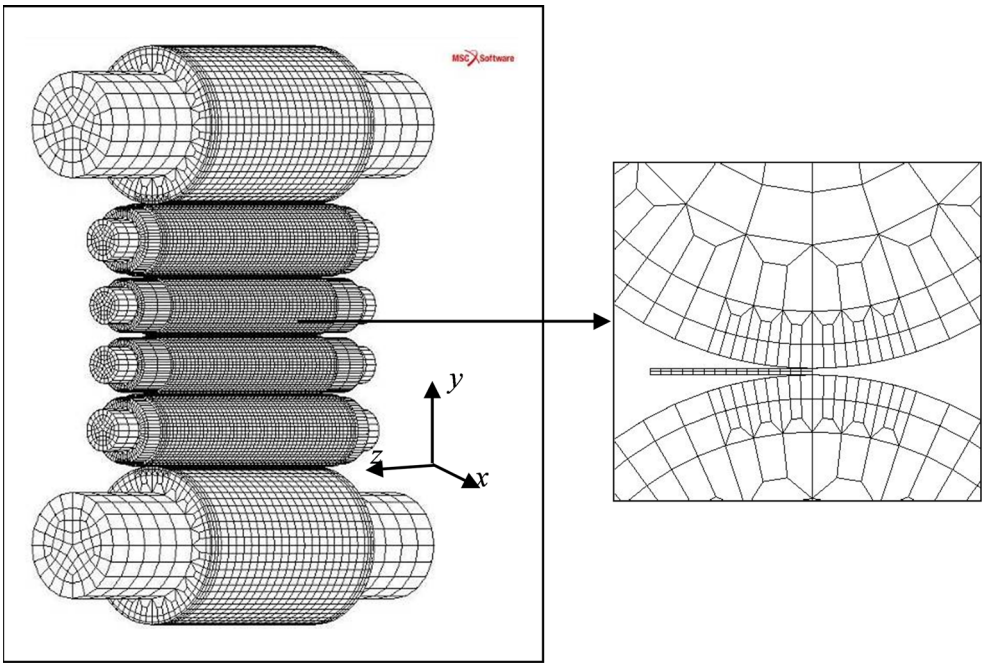

Fig. 3 The 3D FEM for rolls system and strip

capability of entire rolling campaign was improved. Cao et al. [24] built a 3D FEM of roll stacks and strip deformation and analyzed the integrated design of roll contours for strip edge drop and crown control in tandem cold rolling mills. Xu et al. [25] developed a mathematic model to make the relationship between CVC roll contour and the shifting position reasonable, and the optimized CVC work roll contour had obtained good effect in a 1700-mm hot strip mill. Shang et al. [26, 27] found that the shifting position of CVC roll contour was closely related to strip widths and proposed a new CVC work roll contour. However, these optimized contours are not suitable for 6-h CVC cold rolling mill with different strip widths.

In this paper, finite element simulation analysis is conducted to investigate the similarity and complementarity of the main flatness control methods and limitations of flatness defect control. Based on the theoretical and simulated analysis, it tries to address the problem of flatness control capability through roll contour optimization. A segmented CVC intermediate roll contour is proposed and implemented for the production line on the fifth stand, which is considered both narrow strip and ultra-wide strip. This work provides a theoretical basis for the flatness control during the industrial production.

2 The effect function analysis of flatness control

The flatness control of 6-h CVC cold rolling mill essentially controls the flatness stress distribution $\sigma(x)$ of strip through the methods of WRB, IMRB, IMRS, RT, and RSC. The effect function of flatness control method is defined as Eq. (1), which is used to characterize the change capability of flatness stress under the unit adjustment of each control method [15–17]. It is clear that there is consistency between the form of the effect function and flatness stress distribution.

$$\mathrm{Eff}_i(x) = \frac{\Delta\sigma(x)}{\Delta a_i}(i = 1, 2, \cdots n) \tag{1}$$

where x is the width direction coordinates of strip; $\mathrm{Eff}_i(x)$ is the effect function of ith flatness control method; Δa_i is the

Table 1 Key parameters for the FEM

Parameter	Value	Parameter	Value
Work roll body (mm)	ϕ520 × 2180	Work roll neck(mm)	ϕ320 × 610
Intermediate roll body (mm)	ϕ610 × 2580	Intermediate roll neck(mm)	ϕ355 × 430
Backup roll body (mm)	ϕ1400 × 2140	Backup roll neck(mm)	ϕ900 × 630
Roll elasticity modulus (GPa)	210	Roll Poisson ratio	0.30
Strip width (mm)	1000~2000	Strip Poisson ratio	0.28
Strip elasticity modulus (GPa)	210	Friction coefficient	0.03

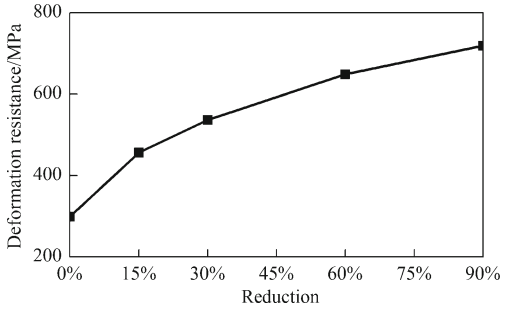

Fig. 4 The stress-strain curve of strip

adjustment valve of *i*th flatness control method; $\Delta\sigma(x)$ is the change of flatness stress along the width direction under the action of flatness control method. When $\Delta\sigma(x)$ is discrete values, the flatness stress change can be expressed by the vector $\Delta\sigma$. Therefore, the effect function can also be expressed by the vector Eff_i.

RT is mainly used to control the asymmetric flatness defects, and RSC is mainly used to control the partial flatness defects, both of which show limited control capability. Therefore, this paper focuses on analyzing the effect function of the three most important and capable flatness control methods for WRB, IMRB, and IMRS.

3 Finite element simulation analysis of strip rolling process in 6-h CVC cold rolling mill

3.1 6-h CVC cold rolling mill parameters and model establishment

A certain 2180 mm CVC tandem cold rolling mill with five stands is anti-symmetrical arranged with the CVC roll contour of upper and lower intermediate rolls (as shown in Fig. 2). Taking the fifth stand which is responsible for the main control task of flatness as the analysis object, and adopting finite element method to obtain the exit strip transverse thickness profile and flatness stress distribution vector σ, a 3D elastic-plastic finite element simulation analysis model, including rolls and strip, is established by using the common MSC.Marc finite element software, as shown in Fig. 3.

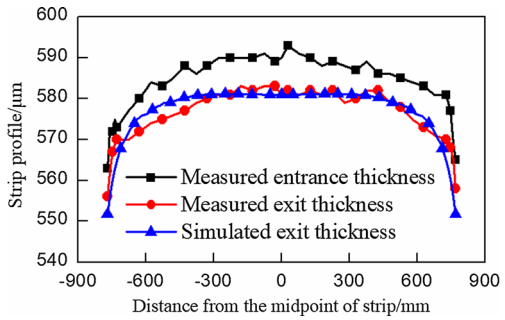

Fig. 5 Verification of the FEM

During the modeling process, each roll contour built as the actual roll contour of the rolling mill, where the work rolls are positive crown roll, the intermediate rolls are five-order CVC roll contour, and the backup rolls are flat roll with rounded edges on both sides. The main geometric and physical parameters are shown in Table 1, and the strip stress-strain curve is shown in Fig. 4. In order to ensure the calculation accuracy of the model, eight nodes and six elements is chosen for the rolls and strip [28, 29]. Plenty of three-dimensional elements are generated as a result of the mesh refinement at the contact interfaces between the rolls and strip. Finally, the number of element of rolls system is 88,212, and element is divided every 5 mm in the width direction and three layers of nodes in the thickness direction for different strip widths.

According to the actual situation of the cold rolling mill and the characteristics of rolling process, the following displacement constraints are imposed on the established FEM: (1) vertical displacement constraints (*y*-direction in Fig. 3) were applied to the neck center of lower backup roll; (2) horizontal displacement constraints (*x*-direction in Fig. 3) were applied to the midpoint of all the roll axes and the *z*-section being zero of strip (the plane of all roll axes); (3) *x*, *y*-direction rotation constraints and *z*-direction displacement constraints were applied to all points on the roll symmetry plane. The FEM is further loaded with the following loads: (1) reduction in the rolling process was applied to the neck center of upper backup roll; (2) WRB force and IMRB force were respectively applied to the neck center of work roll and intermediate roll; (3) entrance and exit tension during the rolling process were certain displacement differences, and were imposed on the entrance and exit sections of strip along the *z*-direction.

3.2 Verification of the FEM and design of simulation conditions

In order to verify the reliability of the FEM, the simulation value of exit strip transverse thickness profile is calculated when the rolling force is 10,520 kN, WRB force is 40 kN, IMRB force is 58.5 kN, IMRS is 8.45 mm, entrance tension is 31 kN, exit tension is 121 kN, strip width is 1550 mm, entrance thickness is 0.59 mm, and rolling exit thickness is 0.581 mm. Compared the strip transverse thickness profile with the actual strip transverse thickness profile from the rolling exit, it can be seen that the profiles are basic coincidence, as shown in Fig. 5.

According to the problem of flatness of different width strips in the production and the urgency of analyzing the flatness control capability of the cold rolling mill, based on the actual process parameters of the fifth stand of 1000 mm, 1500 mm, and 2000 mm strip widths in the production, the simulation conditions are designed, as shown in Table 2. Firstly, the flatness control characteristics of strip width of 1000 mm are analyzed in order to

Table 2 The design of simulation conditions

Strip width (mm)	Reduction (μm)	Exit thickness (mm)	Entrance tension (kN)	Exit tension (kN)	WRB (kN)	IMRB (kN)	IMRS (mm)
1000	2	0.46	16.4	70.4	225	150	100
1500	4	0.7	32.8	147.4	223	147	10
2000	5	0.76	46.3	224.8	205	180	−160

connect the FEM with the actual production process parameters. It is taken 10 kN as a unit adjustment for WRB and IMRB and 1 mm as a unit adjustment for IMRS to simulate and obtain the flatness stress change $\Delta\sigma$ along the strip width, as shown in Fig. 6. The same method is used for the strip widths of 1500 and 2000 mm respectively. The simulated results lay the foundation for the follow-up effect functions of flatness control methods and the adjustability analysis of flatness detects.

4 Analysis of 6-h CVC cold rolling mill flatness control and adjustability of flatness defects

4.1 The effect function of flatness control methods in different strip widths

Combining with the simulated analysis results and Eq. (1), the effect function of each flatness control method can be obtained under the unit adjustment when the strip widths are 1000 mm, 1500 mm, and 2000 mm respectively. At the same time, in order to more directly compare the control effect of the same flatness control method among different strip widths, the strip width $[-B/2, B/2]$ is normalized to $[-1, 1]$ and the flatness stress change is normalized as Eq. (2) [30, 31]. The results are as shown in Fig. 7.

$$f(x) = \frac{\Delta\sigma(x)}{\max|\Delta\sigma(x)|} \tag{2}$$

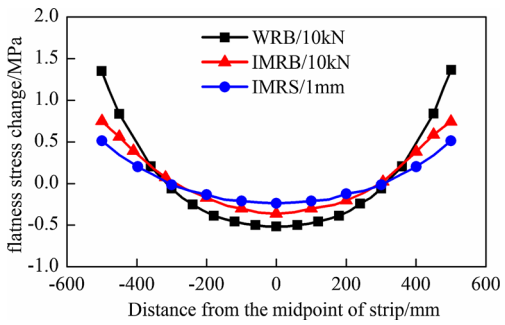

Fig. 6 Calculations of different simulation conditions

where $\max|\Delta\sigma(x)|$ is the maximum values of the variation of flatness stress along width direction under the unit adjustment of each flatness control method.

From Fig. 7a, c, e, it is clear that the control capability of WRB is stronger in the same strip width. As the strip width increases, the flatness stress change of each control method also increases under the unit adjustment. Though the control capability of the same control method is different for different strip widths, from the normalized results, it can be seen from Fig. 7b, d, f that the control effect of each control method is similar, which is consistent with the similar flatness defects of different width strips in the production.

4.2 Similarity and complementarity analysis of the flatness control methods

It can be seen from Fig. 7 that the flatness control methods present some similarities among the effect functions. The relationship among the effect function should be qualitatively and quantitatively analyzed in order to comprehensively master the control capability of the cold rolling mill. Assumed that the cold rolling mill has n kinds of flatness control methods, the effect function of any two different control methods can be presented as Eq. (3):

$$\mathrm{Eff}_2 = a \bullet \mathrm{Eff}_1 + \Delta\mathrm{Eff}_2 \tag{3}$$

where $\Delta\mathrm{Eff}_2$ is the difference between Eff_2 and Eff_1; a is the coefficient to be determined. When $\Delta\mathrm{Eff}_2$ is orthogonal to Eff_1 in Eq. (3), the orthogonal vector set of both can be used to describe the control capability of flatness stress. The Eq. (3) of both sides is multiplied Eff_1, and the result is shown as Eq. (4):

$$a = \frac{1}{|\mathrm{Eff}_1|^2}\mathrm{Eff}_1 \bullet \mathrm{Eff}_2 \tag{4}$$

In the same way, the first two control methods can be used to express the third control method:

$$\mathrm{Eff}_3 = b_1 \bullet \mathrm{Eff}_1 + b_2 \bullet \mathrm{Eff}_2 + \Delta\mathrm{Eff}_3 \tag{5}$$

where $\Delta\mathrm{Eff}_3$ is the difference between Eff_3 and Eff_1, Eff_2; b_1 and b_2 are the coefficient to be determined. Combined with Eqs. (3) and (5), the result is shown as Eq. (6):

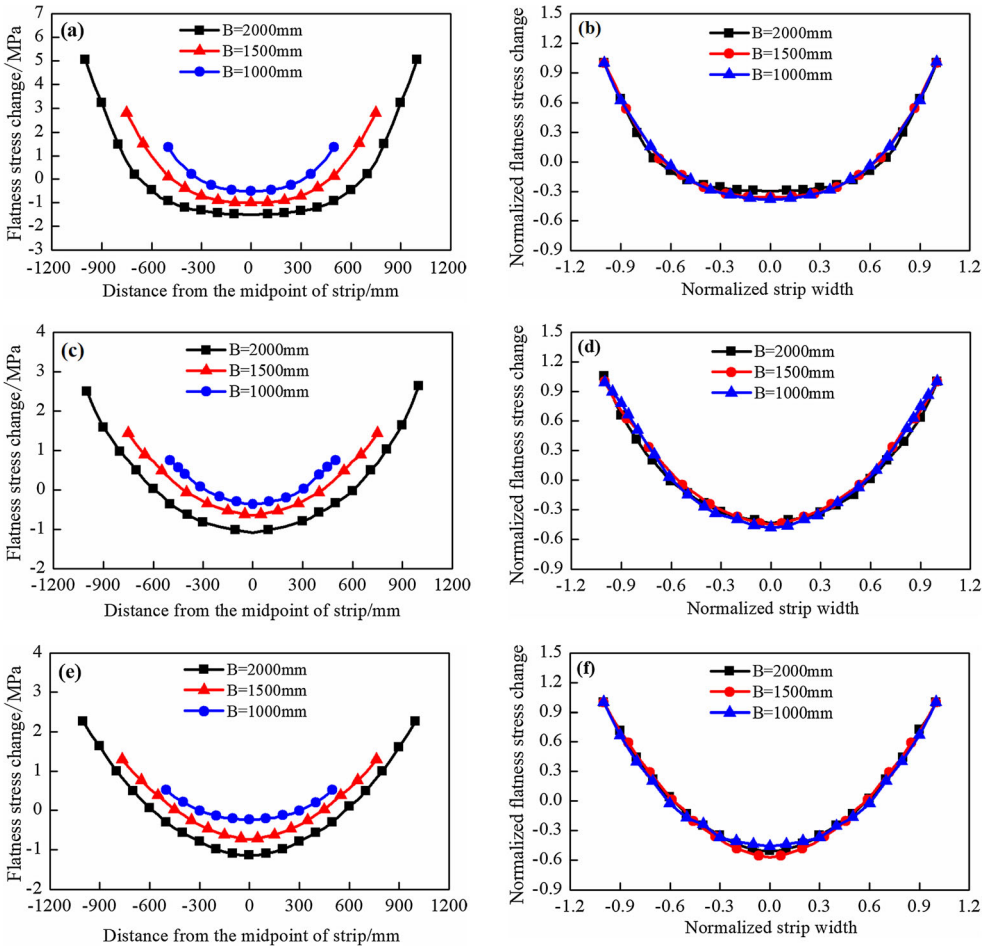

Fig. 7 The effect functions of flatness control methods of different strip widths. **a** The effect function of WRB, **b** the normalized effect function of WRB, **c** the effect function of IMRB, **d** the normalized effect function of IMRB, **e** the effect function of IMRS, **f** the normalized effect function of IMRS

$$\mathrm{Eff}_3 = E \bullet c^T + \Delta\mathrm{Eff}_3 \tag{6}$$

where c is $[b_1 + b_2 a, b_2]$, E is $[\mathrm{Eff}_1, \Delta\mathrm{Eff}_2]$. When $\Delta\mathrm{Eff}_3$ and Eff_1, $\Delta\mathrm{Eff}_2$ are orthogonal, the orthogonal vector of the three can be used to describe the control capability of flatness stress.

The Eq. (6) of both sides is multiplied E^T. The result is shown as Eq. (7):

$$c = \left[\left(E^T \bullet E \right)^{-1} \bullet E^T \bullet \mathrm{Eff}_3 \right]^T \tag{7}$$

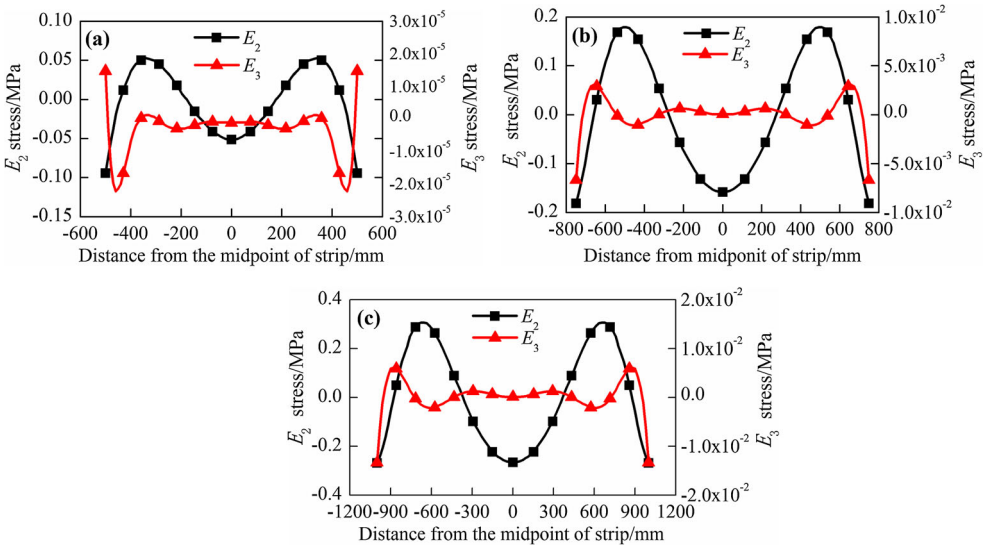

Fig. 8 Flatness control characteristics of different strip widths: **a** The strip width is 1000 mm, **b** the strip width is 1500 mm, **c** the strip width is 2000 mm

Table 3 Similarity and complementarity of flatness control methods of different strip widths

Strip width (mm)	Similarity			Complementarity	
	sim (Eff_1, Eff_2)	sim (Eff_1, Eff_3)	sim (Eff_2, Eff_3)	co_2	co_3
1000	0.990	0.996	0.996	0.141	0.301×10^{-4}
1500	0.981	0.980	0.985	0.194	23.0×10^{-4}
2000	0.982	0.969	0.997	0.189	134×10^{-4}

From Eqs. (3) and (5), it is shown that the cold rolling mill has some similarities among the control methods. Defining $\mathrm{sim}(\mathrm{Eff}_i, \mathrm{Eff}_j)$ as the similarity between the effect functions of any two control methods, the expression of $\mathrm{sim}(\mathrm{Eff}_i, \mathrm{Eff}_j)$ is shown as Eq. (8):

$$\mathrm{sim}\left(\mathrm{Eff}_i, \mathrm{Eff}_j\right) = \frac{\mathrm{Eff}_i \bullet \mathrm{Eff}_j}{|\mathrm{Eff}_i| \bullet |\mathrm{Eff}_j|} \quad (i \neq j) \tag{8}$$

It can be seen that the ith control method not only shows the same flatness control capability as the former i-1 methods, but also has the unique flatness control characteristic $\Delta\mathrm{Eff}_n$. In order to evaluate the unique effect of $\Delta\mathrm{Eff}_n$ in the flatness control process, the complementarity index co_n is defined as Eq. (9):

$$co_i = \frac{|\Delta \mathrm{Eff}_i|}{|\mathrm{Eff}_i|} \quad i \geq 2 \tag{9}$$

WRB presents strongest control capability in the analysis of Section 4.1. This work applies Eff_1, Eff_2, and Eff_3 to express the effect functions of WRB, IMRB, and IMRS, which are calculated in Section 4.1. In order to analyze and describe conveniently, the effect function of WRB is expressed as E_1; the differences ΔEff_2 between IMRB and WRB is expressed as E_2; the difference ΔEff_3 between IMRS and both of WRB and IMRB is expressed as E_3. E_2 and E_3 are calculated by Eqs. (3) ~ (7), as shown in Fig. 8. Regarding the different strip widths, it can be seen that the flatness control characteristics E_2 and E_3 increase with the strip width. For same strip width, the value of E_2 is obviously greater than the value of E_3 along the width direction. The set of orthogonal vectors E_1, E_2, and E_3 is named as eigenvectors, which is to describe the flatness control characteristic of the cold rolling mill.

Using Eq. (8) to calculate the similarities between any two control methods of WRB, IMRB, and IMRS, as shown in Table 3. It can be seen that the similarities between any two different control methods reach more than 0.96 in different strip widths. From Eq. (9), the complementarity of IMRB and IMRS can be presented as Eq. (10):

$$co_i = \frac{|\Delta \mathrm{Eff}_i|}{|\mathrm{Eff}_i|} = \frac{|E_i|}{|\mathrm{Eff}_i|} \quad i = 2, 3 \tag{10}$$

The complementarities of two control methods of IMRB and IMRS are calculated by E_2 and E_3, both of which are less than 0.2 in different strip widths, as shown in Table 3. The complementarity of IMRS is extremely low. It indicates that the cold rolling mill obtains three typical flatness control methods, but the similarities between three control methods are too high that only work on the same flatness defects. In particular, although IMRS has a strong capability to control roll gap crown, the complementarity with WRB, IMRB is still poor, which makes it difficult to address the typical flatness defects.

4.3 Adjustability analysis of the flatness defects

Based on the analysis of control flatness capability above, as well as combined with the actual flatness defects from the industrial production, the control capability of typical flatness defects is further analyzed. Before the control is applied, if the

Table 4 The similarity between flatness stress and eigenvectors and the elimination degrees of flatness defects

Strip width (mm)	Flatness stress (MPa)	Similarity			Degrees of the flatness defects
		E_1	E_2	E_3	α
1000	σ_1	−0.114	−0.009	−0.052	0.79%
	σ_2	0.190	0.281	0.241	9.07%
1500	σ_1	0.181	0.312	0.294	11.49%
	σ_2	0.194	0.361	0.327	14.85%
2000	σ_1	0.205	0.338	0.374	16.10%
	σ_2	0.371	0.541	0.567	50.28%

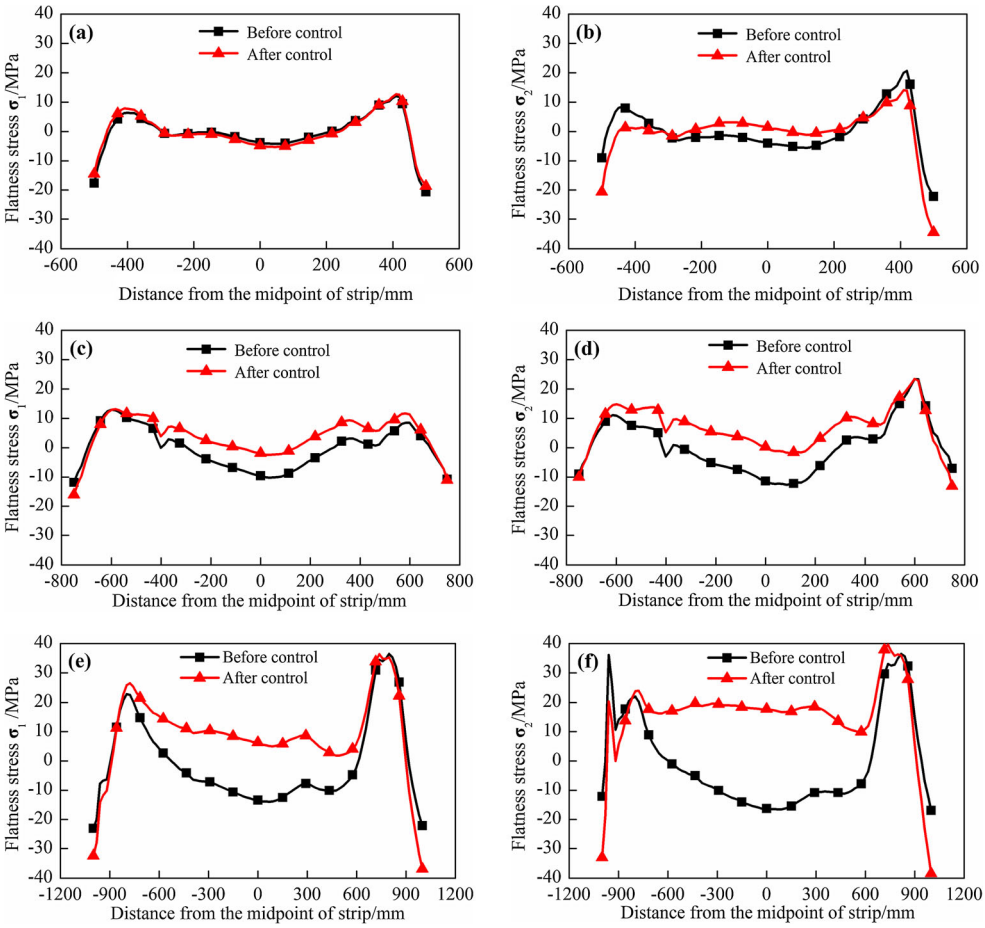

Fig. 9 Comparison of the flatness stress before and after control of different strip widths: **a**, **b** The strip width is 1000 mm; **c**, **d** the strip width is 1500 mm; **e**, **f** the strip width is 2000 mm

flatness stress is σ_0 along the strip width direction, the controlled flatness stress $\Delta\sigma_0$ can be expressed as Eq. (11):

$$\Delta\sigma_0 = \sigma_0 - \sum_{i=1}^{n} \Delta a_i \times \mathrm{Eff}_i(\, i = 1, 2, 3) \tag{11}$$

According to the method of least square method [32], the square of the controlled flatness stress $\Delta\sigma_0$ can be further calculated as Eq. (12):

$$|\Delta\sigma_0|^2 = |\sigma_0|^2 \left[1 - \sum_{i=1}^{n} \mathrm{sim}^2(\sigma_0, E_i)\right] \tag{12}$$

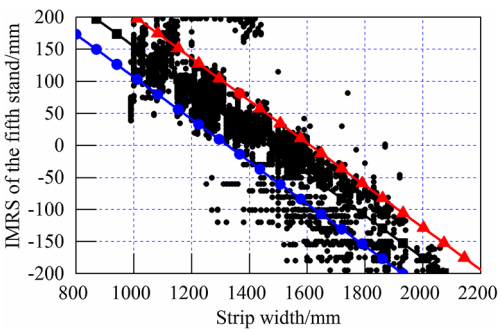

Fig. 10 The relationship between strip widths and IMRS of the fifth stand

where $\mathrm{sim}(\sigma_0, E_i)$ is the similarity of σ_0 and E_i. If $|\sigma_0|$ is known, it can be seen that the square of $|\Delta\sigma_0|$ and the square sum of $\mathrm{sim}(\sigma_0, E_i)$ is negatively linear. The smaller sum of squares of $\mathrm{sim}(\sigma_0, E_i)$, the closer $|\Delta\sigma_0|$ and $|\sigma_0|$, which indicates that the current flatness control methods of the cold rolling mill cannot effectively control the flatness defects.

In order to more intuitively describe the control capability of the cold rolling mill for the flatness defects, the flatness defect elimination degree α is defined as follows Eq. (13):

$$\alpha = 1 - \frac{|\Delta\sigma_0|}{|\sigma_0|} = \left(1 - \sqrt{1 - \sum_{i=1}^{n} \mathrm{sim}(\sigma_0, E_i)^2}\right) \times 100\% \tag{13}$$

According to the data mining theory, the proposed method of cluster analysis for strip flatness stress characteristics grid shape and density is used to extract the flatness stress characteristics of different strip width of 2180 mm cold rolling mill and then the adjustability of flatness stress characteristics are analyzed [33, 34]. On the basis of the concept of "big data," the flatness stress σ_1 and flatness stress σ_2 essentially present two different forms of stress distribution of the same strip width. From Eq. (13), the similarities between flatness stress σ_i ($i = 1,2$) and eigenvectors E_i ($i = 1,2,3$), and the flatness

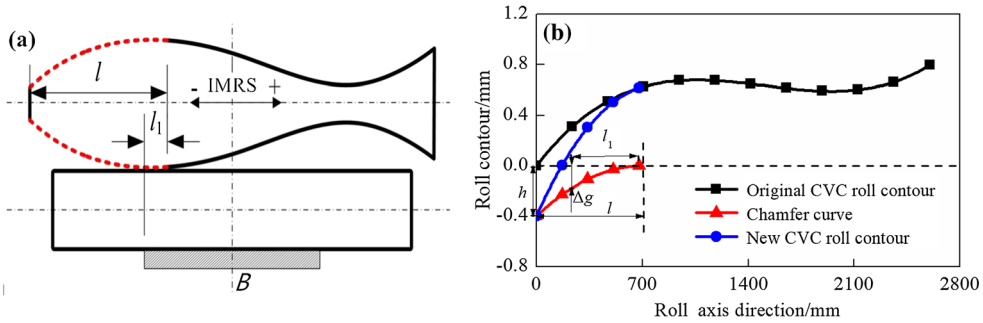

Fig. 11 Segmented CVC intermediate roll contour: **a** The diagram of roll contour, **b** roll contour design method

defect elimination degree α are calculated in different strip widths of 1000 mm, 1500 mm, and 2000 mm, as shown in Table 4. It can be seen that except for the defect elimination degree of flatness stress σ_2 of strip width of 2000 mm reaching 50%, the flatness defect elimination degrees of the other strip widths are no more than 16%.

Through the analysis above, the flatness stress before and after control of different strip widths are compared, as shown in Fig. 9. It can be seen from Fig. 9a that the flatness stress σ_1 is hardly improved and from Fig. 9b, the flatness stress σ_2 shows a more serious edge waves. From Fig. 9c, d, it can be seen that the center waves are basically controlled, while the edge waves are not improved at all. From Fig. 9e, f, it can be seen that although the center waves can be significantly improved, the coupled edge and center waves of strip are converted to more serious edge waves. It is clear that the overall flatness defects cannot be improved in different strip widths. Thus, the current 2180 mm tandem cold mill with flatness control methods is really difficult to control complex waves, which appear in the production of both narrow strip and ultra-wide strip.

5 Segmented CVC roll contour optimization and industrial experiment

5.1 IMRS characteristic of CVC roll contour

Based on data analysis in the industrial production, it is found that the value of IMRS is greatly affected by the change of strip widths. Taking the strip widths as the variable, a large number of statistics is made on IMRS positions of the fifth stand and strip widths (as shown in Fig. 10). It is found from Fig. 10 that there is a clear correspondence between IMRS and strip widths. By using the numerical analysis to linearize the channeling data of different width strips, it can be seen that more than 90% IMRS fall in the regression line deviation of ± 50 mm channeling range. The relationship between strip width B and IMRS can be expressed as Eq. (14):

$$-0.327B + 433.152 \le IMRS \le -0.327B + 533.152 \quad (14)$$

From the Fig. 10, it can be further found that the positive and negative IMRS are basic to the limit, which shows the cold rolling mill is lack of control capability for the coupled edge and center waves when the strip width is less than 1300 mm or more than 1700 mm. Therefore, it can be seen whether the adjustability analysis of flatness defects based on the effect function or the analysis of relationship between IMRS and strip widths, the 2180 mm cold tandem mill is difficult to control the flatness defects and especially control the flatness defects of strip edges with different strip widths under the existing roll contour configuration.

5.2 Segmented CVC intermediate roll contour optimization

For a certain mill, roll contour optimization is the most direct and effective means to control flatness defects [35-37].

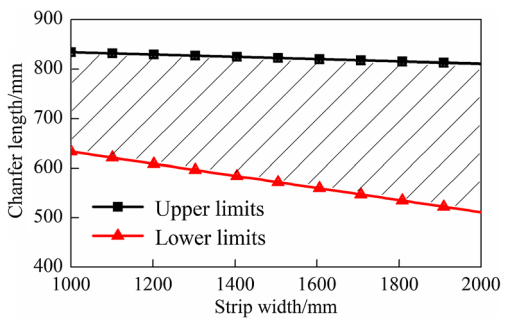

Fig. 12 The range of chamfer length l

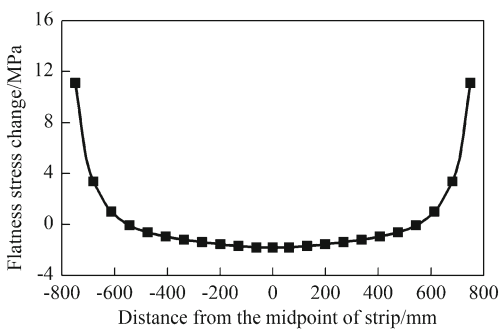

Fig. 13 The effect function of chamfer depth

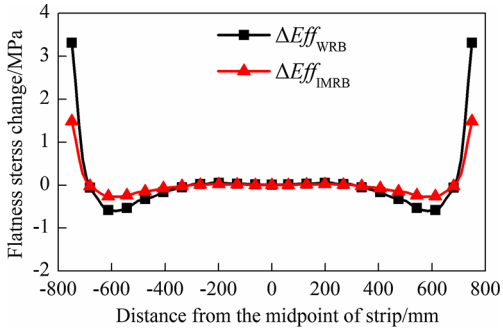

Fig. 14 Chamfer depth influence on the effect function of WRB and IMRB

Combined with the corresponding relationship between IMRS of the fifth stand and strip widths (as shown in Fig. 10), a new local edge wave control capability of variable crown intermediate roll contour is proposed which aims to convert the coupled edge and center wave defects into center wave defects. Then, the converted waves can be eliminated by using the existing flatness control methods. The specific method for optimizing the roll contour is as follows: a contour called a chamfer curve is superimposed on the end of intermediate roll, which is determined by the chamfer length l, curve form y_1 and chamfer depth h. The available length of chamfer in the strip is l_1 and the corresponding chamfer depth is Δg when the strip width is determined (as shown in Fig. 11). The chamfer length is determined by Eq. (15). The curve form y_1 is expressed by Eq. (16) in order to ensure that the roll contour curve is smooth and continuous with the original roll contour curve after superposition at the boundary.

$$l = l_1 + \frac{1}{2}(l_{\mathrm{IMR}} - B) + IMRS \tag{15}$$

$$y_1 = b_0(x - l)^2 \tag{16}$$

where l is the chamfer length; l_1 is the available length of chamfer in the strip; l_{IMR} is the body length of intermediate roll; b_0 is the coefficient to be determined; x is the distance from cone end.

The relationship among roll body length l_{IMR}, strip width B and corresponding IMRS is known from Eqs. (15) and (16). If the relationship between available length l_1 and strip width B is determined, the chamfer length l can be determined. From the flatness stress σ_i $(i = 1, 2)$ of different strip widths shown in Fig. 9, it can be seen that the localized peaks of flatness stress are within 0.2 ± 0.1 times $B/2$ of the strip edge. Therefore, if the intermediate roll segmented roll contour is used to control the strip edge flatness, the segmented available length l_1 should be matched with the scope of local peaks. The available length l_1 can be expressed as Eq. (17):

$$\frac{B}{20} \le l_1 \le \frac{3B}{20} \tag{17}$$

Combined with Eqs. (14), (15), and (17), the range of chamfer length l can be obtained as shown in Eq. (18) and Fig. 12.

$$-0.123B + 756.848 \le l \le -0.023B + 856.848 \tag{18}$$

Considering that the chamfer length cannot be modified in the rolling process and the margin for the subsequent optimization of chamfer can be reserved, the chamfer length l is selected as 700 mm. From Eq. (16), the chamfer curve can be determined by using the segmented length l_1 and the corresponding chamfer depth Δg when the chamfer length l is determined. Taking chamfer depth Δg 10 μm as a unit adjustment, the new roll contour is put into the established FEM to calculate the effect function Eff$g$ of chamfer available depth under the unit adjustment when the strip is 1500 mm mentioned above, as shown in Fig. 13. Denoting the corresponding influence on the effect functions of WRB and IMRB as $\Delta\mathrm{Eff}_{\mathrm{WRB}}$ and $\Delta\mathrm{Eff}_{\mathrm{IMRB}}$ respectively, the results are as shown in Fig. 14.

The similarities of flatness stress σ_2 between $\Delta\mathrm{Eff}_{\mathrm{WRB}}$ and $\Delta\mathrm{Eff}_{\mathrm{IMRB}}$ are 0.68 and 0.59 respectively when the strip width is 1500 mm (as shown in Fig. 9d). Compared with the original CVC roll contour, the flatness defect elimination degree increases from 14.85 to 56%. It shows that the new CVC roll contour not only adds the control capability Effg but also strengthens the control capability of WRB and IMRB on strip edges, which makes it possible to control complex flatness defects for the 2180 mm cold rolling mill.

The chamfer available segmented length l_1 and chamfer depth Δg vary with IMRS because of strip width changes. Taking the strip widths of 1000 mm, 1500 mm, and 2000 mm as examples, the optimal chamfer depth Δg is obtained and the corresponding coefficient b_0 and chamfer depth

Table 5 The parameters of intermediate roll chamfer curve of different strip widths

Strip width (mm)	IMRS (mm)	l_1 (mm)	Δg (μm)		b_0 (μm)		H (μm)	
			σ_1 (MPa)	σ_2 (MPa)	σ_1 (MPa)	σ_2 (MPa)	σ_1 (MPa)	σ_2 (MPa)
1000	150	135	14.152	14.355	7.765×10^{-4}	7.877×10^{-4}	380.493	385.951
1500	− 10	175	24.835	24.988	8.273×10^{-4}	8.159×10^{-4}	405.360	399.808
2000	− 180	230	43.138	44.184	8.163×10^{-4}	8.344×10^{-4}	400.003	408.840

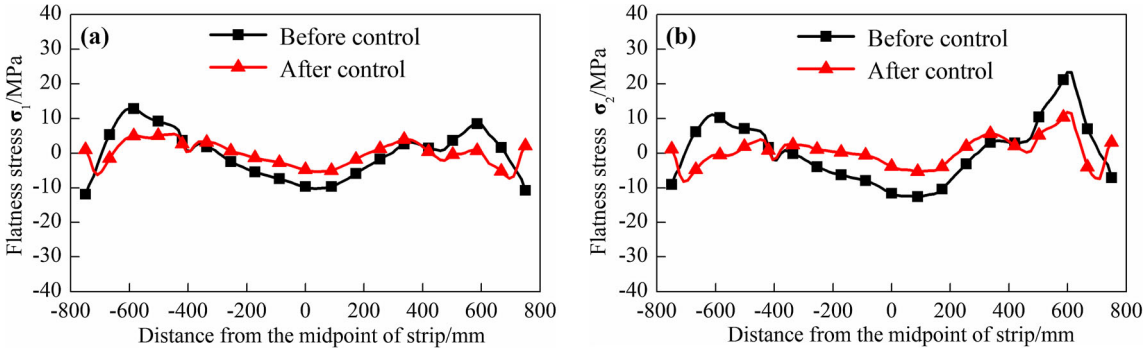

Fig. 15 Comparison of the flatness stress before and after control: **a** flatness stress σ_1; **b** flatness stress σ_2

h are obtained from Eq. (16), as shown in the Table 5. It can be seen that the chamfer depths h of different strip widths are relatively close. The chamfer depth h is applied as 400 μm to match the control of flatness defects on strip edges with different widths.

In order to verify the feasibility of the new CVC roll contour, the flatness control effect is further analyzed when the strip width is 1500 mm, as shown in Fig. 15. It can be seen from Fig. 15 that the strip edge flatness is effectively controlled and the center flatness defect is also controlled on some extents. The corresponding flatness value of flatness stress σ_1 is reduced from 2.8 to 1.8 IU, and the corresponding flatness value of flatness stress σ_2 is reduced from 3.6 to 1.6 IU. It is further demonstrated that the new CVC roll contour has the potential to effectively control the flatness defects of strip edges and improve the overall flatness quality.

5.3 Industrial experiment

To verify the flatness control effect of the new CVC roll contour for 2180 mm tandem cold mill with different width strips, an industrial production experiment has been carried out. The new CVC roll contour is installed on the fifth stand. At the same time, replacing work rolls of five stands is prepared to ensure stable production without downtime for replacing intermediate roll. During production, the rolled strip width distribution of the new CVC roll contour is shown in Fig. 16, a total of 266 strip coils, which cover about 80% of the strip width specifications of the 2180 mm tandem cold rolling mill.

The rolling process with different strip widths is tracked during production. And the actual flatness stress distribution of different strip widths is compared and analyzed under original CVC roll contour and new CVC roll contour, as shown in Fig. 17. It can be seen from Fig. 17a that the deviation of flatness stress is reduced from 40 MPa to less than 20 MPa within 200 mm from the edge of both driving side (DS) and operating side (OS). From Fig. 17b, it can be seen that the deviation of flatness stress is reduced from 76 to 32 MPa within 200 mm of the DS. From Fig. 17c, it can be seen that the deviation of flatness stress is reduced from 81 to19 MPa within 200 mm of the DS, and the deviation of flatness stress is reduced from 49 to 20 MPa within 200 mm of the OS. It is shown that the edge flatness has been improved of different strip widths. The actual flatness stress of 100 strip coils is collected and analyzed for different strip widths under the original CVC roll contour and the new CVC roll contour. It is found that the proportion of coupled edge

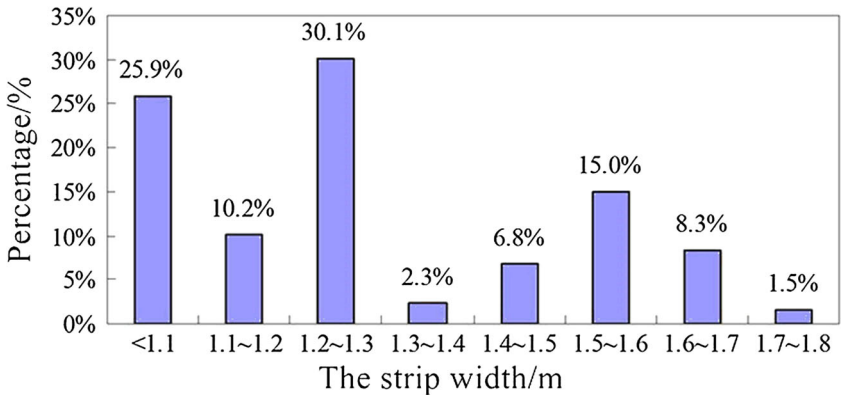

Fig. 16 Rolled strip widths distribution during the new CVC roll contour production

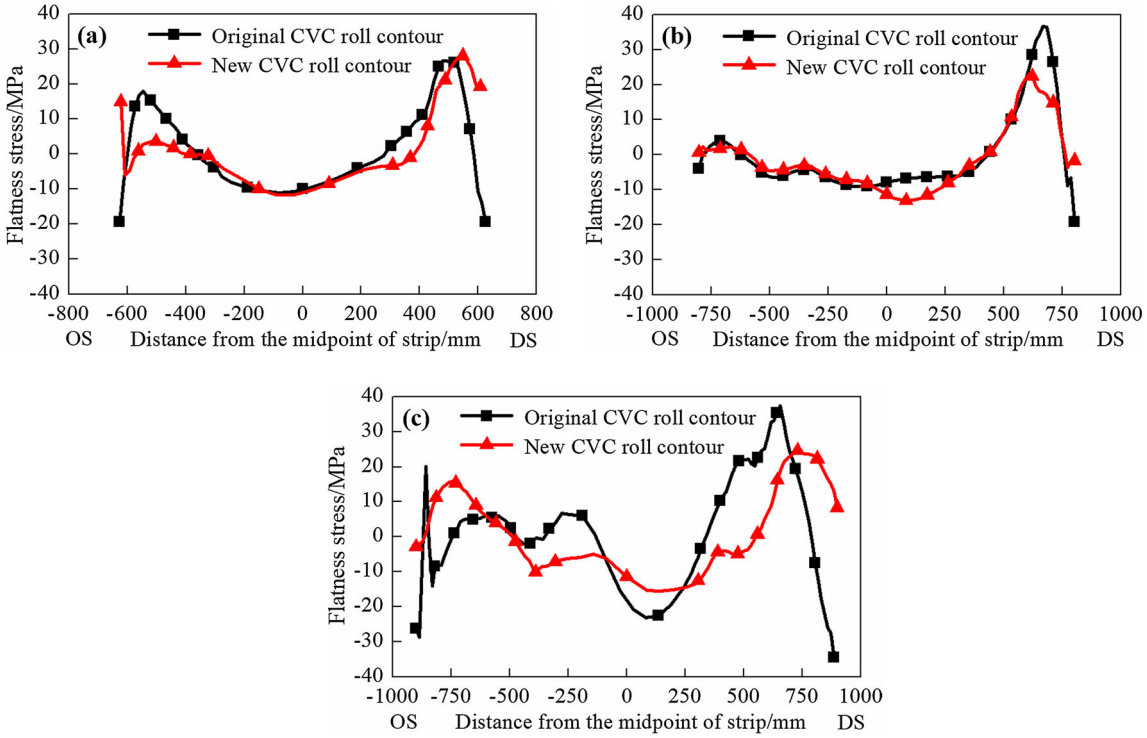

Fig. 17 Comparison of actual flatness characteristics of different strip widths: **a** the strip width is 1254 mm, **b** the strip width is 1605 mm, **c** the strip width is 1800 mm

and center waves decreases by 15.2% and the average flatness decreases by 0.7 IU. The quality of rolled strip flatness has been improved with proposed contour.

6 Conclusion

(1) The importance and limitations of flatness control capability is analyzed simply for the 6-h CVC cold rolling mill. An integrated 3D elastic-plastic FEM of rolls system and strip is built by using the MSC.Marc software, and the effect functions of WRB, IMRB, and IMRS under a unit adjustment are calculated. The control capability of each control method is clarified for different strip widths.

(2) From qualitatively and quantitatively analysis of the effect functions, it is found that the effect functions of the similarities between any two kinds of flatness control methods are more than 0.96, but the complementarities are less than 0.20. In particular, IMRS has very low complementarity with the WRB, IMRB and decreases as the strip width decreases. The relationship between different flatness control methods is further clarified, and a set of orthogonal vectors defined as eigenvectors is proposed for describing 6-h CVC cold rolling mill flatness control characteristics.

(3) According to the analysis of flatness defects in the industrial production, the flatness defects can be eliminated is influenced by the similarity between flatness stress and eigenvectors. The low similarity between each other makes it difficult to eliminate the flatness defects, especially for edge waves. The root reason why the cold rolling mill cannot control the coupled center and edge waves is found. The research results provide theoretical basis for explaining the flatness control problems in the industrial production.

(4) Combined with the theoretical analysis and the actual situation in the production, a segmented CVC intermediate roll contour is proposed, which enhances the control capability of 6-h CVC cold rolling mill on the flatness. The new CVC roll contour has been implemented in the production line on the fifth stand. The proportion of coupled edge and center waves decreases by 15.2%. The average flatness reduces by 0.7 IU.

Funding information This work is supported by “the National Key Technology R&D Program of the 12th Five-year Plan of China” (grant no. 2015BAF30B01) and “the Fundamental Research Funds For the central Universities” (grant no. FRF-BR-16-025A, FRF-TP-15-016A3). The authors also thank Wuhan Iron & Steel (Group) Corp. for the industrial experiments and financial support.

References

1. Wang XD, Li F, Li BH, Dong LJ, Zhang BH (2012) Design and application of an optimum backup roll contour configured with CVC work roll in hot strip mill. ISIJ Int 52:1637–1643. https://doi.org/10.2355/isijinternational.52.1637
2. Ginzburg VB, Ballas R (2000) Flat roll fundamentals. Marcel Dekker, Inc., New York
3. Linghu KZ, Jiang ZY, Zhao JW, Li F, Wei DB, Xu JZ, Zhang XM, Zhao XM (2014) 3D FEM analysis of strip shape during multi-pass rolling in a 6-high CVC cold rolling mill. Int J Adv Manuf Technol 74:1733–1745. https://doi.org/10.1007/s00170-014-6069-z
4. Huang HG, Shi YQ, Ren XY, Du FS (2014) Influence of initial crown of work roll on strip shape adjusting performance of ultra-wide 6-h CVC mill. Iron and Steel 49:88–93. https://doi.org/10.13228/j.boyuan.issn0449-749x.2014.07.004
5. Linghu KZ, Jiang ZY, Li F, Zhao JW, Yu M, Wang YQ (2014) FEM analysis of profile control capability during rolling in a 6-high CVC cold rolling mill. Adv Mater Res 988:257–262. https://doi.org/10.4028/www.scientific.net/AMR.988.257
6. Liu HM, Zheng ZZ, Peng Y (2000) Computer simulation of the roll contact pressure character for 6-high CVC wide strip mill. Journal of Mechanical Engineering 36:69–73
7. Li HB, Zhang J, Cao JG, Cheng FW, Hu WD, Zhang Y (2012) Roll contour and strip profile control characteristics for quintic CVC work roll. Journal of Mechanical Engineering 48:24–30
8. Yang GH, Zhang J, Cao JG, Li HB, Huang QB (2016) Effect of different stands of 2180mm tandem cold rolling mill on shape control of products. J Beijing Inst Technol 36:1111–1116. https://doi.org/10.15918/j.tbit1001-0645.2016.11.003
9. Bao RR, Zhang J, Li HB, Jia SH, Liu HJ, Li XJ (2015) Influence of asymmetric flatness errors on strip wandering in continuous annealing lines. Iron and Steel 50:35–38. https://doi.org/10.13228/j.boyuan.issn0449-749x.20140726
10. Zhang QD, Huang LW, Zhou XM (2000) Comparative study on shape control technologies for wide strip mill. J Univ Sci Technol Beijing 22:177–181. https://doi.org/10.13374/j.issn100-053x.2000.02.023
11. Wang RZ, He AR, Yang Q, Zhao L, Dong HR (2006) Profile control capability of LVC work roll contour. Iron Steel 41:41–44. https://doi.org/10.13228/j.boyuan.issn0449-749x.2006.05.010
12. Wang QL, Sun J, Li X, Liu YM, Wang PF, Zhang DH (2018) Numerical and experimental analysis of strip cross-directional control and flatness prediction for UCM cold rolling mill. J Manuf Process 34:637–649. https://doi.org/10.1016/j.jmapro.2018.07.008
13. Rosenthal D (1988) CVC technology on hot and cold strip rolling mills. Rev Met Cahiers D'Inform Tech 85:597–606. https://doi.org/10.1051/metal/198885070597
14. Bald W, Klamma K (1988) CVC technology for cold rolling mills-plant examples. Iron Steel Eng 65:24–28
15. Wang CS, Zhang YP, Zhang QD (1999) Application of evaluation function in cold mill shape control. Steel Rolling 4:28–30. https://doi.org/10.13228/j.boyuan.issn1003-9996.1999.04.011
16. Zhang YP, Wang CS (1999) Flatness control strategy on cold mill based on efficiency function. J Univ Sci Technol Beijing 21:195–197. https://doi.org/10.13374/j.issn100-053x.1999.02.056
17. Liu HM, Zhang XL, Wang YR (2005) Transfer matrix method of flatness control for strip mills. J Mater Process Technol 166:237–242. https://doi.org/10.1016/j.jmatprotec.2004.08.018
18. Song L, Shen MG, Yang LP, Liu J, Wang JS, Chen XB (2016) Shape control dimensionality reduction efficiency inherited regulation method of cold rolling wide strip. Iron Steel 51:70–75. https://doi.org/10.13228/j.boyuan.issn0449-749x.20150083
19. Yan QT, Zhang J, Jia SH, Chu YG, Yang GH, Gong Y (2011) Research on analyzing the flatness adjusting capacity for cold mill and its application. J Mech Eng 47:77–81. https://doi.org/10.3901/JME.2011.04.077
20. Ataka M (2015) Rolling technology and theory for the last 100 years: the contribution of theory to innovation in strip rolling technology. ISIJ Int 55:89–102. https://doi.org/10.2355/isijinternational.55.89
21. Moazeni B, Salimi M (2015) Investigations on relations between shape defects and thickness profile variations in thin flat rolling. Int J Adv Manuf Tech 77:1315–1331. https://doi.org/10.1007/s00170-014-6544-6
22. Lu C, Tieu AK, Jiang ZY (2002) A design of a third-order CVC roll profile. J Mater Process Technol 125:645–648. https://doi.org/10.1016/S0924-0136(02)00373-4
23. Li YL, Cao JG, Qiu L, Yang GH, He AR, Zhou YZ (2018) Research on ASR work roll contour suitable for all width electrical steel strip during hot rolling process. Int J Adv Manuf Tech 97:3453–3458. https://doi.org/10.1007/s00170-018-2198-0
24. Cao JG, Chai XT, Li YL, Kong N, Jia SH, Zeng W (2017) Integrated design of roll contours for strip edge drop and crown control in tandem cold rolling mills. J Mater Process Technol 252:432–439. https://doi.org/10.1016/j.jmatprotec.2017.09.038
25. Xu G, Liu XJ, Zhao JR, Xiong JW (2007) Analysis of CVC roll contour and determination of roll crown. J Univ Sci Technol Beijing 14:378–380. https://doi.org/10.1016/S1005-8850(07)60075-9
26. Shang F, Li HB, Kong N, Zhang J, Hu C, Zhang C, Chen JF, Mitchell DRG (2017) Improvement in continuously variable crown work roll contour under CVC cyclical shifting mode. Int J Adv Manuf Technol 90:2723–2731. https://doi.org/10.1007/s00170-016-9587-z
27. Shang F, Li HB, Kong N, Zhang J, Hu C, Chen L, Zhang C, Chen JF (2016) CVC cyclical shifting mode and its working characteristics for the mills of CSP. Int J Adv Manuf Technol 87:1906–1917. https://doi.org/10.1007/s00170-016-8602-8
28. Park H, Hwang S (2017) 3-D coupled analysis of deformation of the strip and rolls in flat rolling by FEM. Steel Res Int 88:1700227. https://doi.org/10.1002/srin.201700227
29. Yu HL, Tieu K, Lu C, Deng GY, Liu XH (2013) Occurrence of surface defects on strips during hot rolling process by FEM. Int J Adv Manuf Technol 67:1161–1170. https://doi.org/10.1007/s00170-012-4556-7
30. Bao RR, Zhang J, Li HB, Jia SH, Liu HJ, Xiao S (2015) Flatness pattern recognition of ultra-wide tandem cold rolling mill. Chin J Eng 37:6–11. https://doi.org/10.13374/j.issn2095-9389.2015.s1.002
31. Niu PF, Liu C, Li PF, Li GQ (2014) Optimized support vector regression model by improved gravitational search algorithm for flatness pattern recognition. Neural Comput Appl 26:1167–1177. https://doi.org/10.1007/s00521-014-1798-3
32. Chen XR (1998) Historical backgrounds and present state of the least squares method. J Univ Chin Acad Sci 15:4–11
33. Li HB, Bao RR, Zhang J, Jia SH, Chu YG, Liu HJ (2016) Cluster analysis of strip flatness characteristics for ultra-wide cold rolling mill. Chin J Eng 38:1569–1575. https://doi.org/10.13374/j.issn2095-9389.2016.11.009
34. Ester M, Kriegel HP, Sander J, Xu XW (1996) A density-based algorithm for discovering clusters in large spatial databases with noise. In: The Second International Conference on Knowledge Discovery and Data Mining (KDD-96), Portland, USA
35. Li HB, Zhang J, Cao JG, Wang ZM, Wang Q, Zhang SS (2010) Analysis and selection of crown control ranges for CVC work rolls in CSP hot rolling. J Univ Sci Technol Beijing 32:118–122. https://doi.org/10.13374/j.issn1001-053x.2010.01.002
36. Liu GM, Di HS, Guang A (2008) Discussion on design of CVC roll profile and its equivalent crown. J North Univ 29:1443–1446
37. Wei GC, Cao JG, Zhang J, Hai JW, Chen G (2007) Optimization and application of CVC work roll contour on 2250 hot strip mills. J Cent South Univ 38:937–942